Control-Oriented Model With Intra-Patient Variations for an Artificial Pancreas

Marcela Moscoso-Vásquez, Patricio Colmegna, Nicolás Rosales, Fabricio Garelli, and Ricardo Sánchez-Peña, *Senior Member, IEEE*

***Abstract*—In this work, a low-order model designed for glucose regulation in Type 1 Diabetes Mellitus (T1DM) is obtained from the UVA/Padova metabolic simulator. It captures not only the nonlinear behavior of the glucose-insulin system, but also intra-patient variations related to daily insulin sensitivity (S_I) changes. To overcome the large inter-subject variability, the model can also be personalized based on *a priori* patient information. The structure is amenable for linear parameter varying (LPV) controller design, and represents the dynamics from the subcutaneous insulin input to the subcutaneous glucose output. The efficacy of this model is evaluated in comparison with a previous control-oriented model which in turn is an improvement of previous models. Both models are compared in terms of their open- and closed-loop differences with respect to the UVA/Padova model. The proposed model outperforms previous T1DM control-oriented models, which could potentially lead to more robust and reliable controllers for glycemia regulation.**

***Index Terms*—Intra-patient variations, LPV model, type 1 diabetes, control-oriented model, artificial pancreas.**

Manuscript received August 16, 2019; revised December 12, 2019; accepted January 16, 2020. Date of publication January 27, 2020; date of current version September 3, 2020. This work was supported by Nuria (Argentina) and Cellex (Spain) Foundations, by CONICET (PIP-0837), ANPCyT (PICT-3211), and JDRF (2-APF-2019-737-A-N). Funding sources had no active involvement in the development of this work. *(Corresponding author: Marcela Moscoso-Vásquez.)*

M. Moscoso-Vásquez is with the Centro de Sistemas y Control, Instituto Tecnológico de Buenos Aires (ITBA), Buenos Aires, C1106ACD, Argentina, and also with the Consejo Nacional de Investigaciones Científicas y Técnicas (CONICET), Buenos Aires, C1425FQB, Argentina (e-mail: mmoscoso@itba.edu.ar).

P. Colmegna is with the Center for Diabetes Technology, University of Virginia (UVA), Charlottesville, VA 22903 USA, and with the Departamento de Ciencia y Tecnología, Universidad Nacional de Quilmes (UNQ), Bernal, B1876, Argentina, and also with the Consejo Nacional de Investigaciones Científicas y Técnicas (CONICET), Buenos Aires, C1425FQB, Argentina (e-mail: pc2jx@virginia.edu).

N. Rosales is with the LEICI, Universidad Nacional de La Plata–CONICET, La Plata, B1900, Argentina (e-mail: nicolas.rosales@ing.unlp.edu.ar).

F. Garelli is with the LEICI, Universidad Nacional de La Plata–CONICET, La Plata, B1900, Argentina, and also with the Consejo Nacional de Investigaciones Científicas y Técnicas (CONICET), Buenos Aires, C1425FQB, Argentina (e-mail: fabricio@ing.unlp.edu.ar).

R. Sánchez-Peña is with the Centro de Sistemas y Control, Instituto Tecnológico de Buenos Aires (ITBA), Buenos Aires, C1106ACD, Argentina, and also with the Consejo Nacional de Investigaciones Científicas y Técnicas (CONICET), Buenos Aires, C1425FQB, Argentina (e-mail: rsanchez@itba.edu.ar).

Digital Object Identifier 10.1109/JBHI.2020.2969389

I. Introduction

TYPE 1 Diabetes Mellitus (T1DM) is a chronic disease characterized by an absolute insulin deficit, and therefore, patients rely on exogenous insulin dosage to achieve glucose regulations and avoid complications such as hypo- or hyperglycemia and their long-time adverse effects.

The Artificial Pancreas (AP) is a system conceived to automate the exogenous insulin supply by usually connecting a Continuous Glucose Monitoring (CGM) sensor with a subcutaneous insulin pump through a control algorithm. The core of the AP is the control algorithm, which estimates the amount of insulin to be administered to the patient. The main challenge to achieve good Blood Glucose (BG) control is that each patient can be characterized by nonlinear dynamics with time-varying parameters and responses that change not only from one person to another (inter-subject variability), but also from day to day for the same person (intra-subject variability). Therefore, the control algorithm must be designed with robustness and time-varying properties to make closed-loop control reliable and safe [1]–[3].

Inter-patient variations are mostly related to differences in Insulin Sensitivity (S_I), requirements and absorption/action times [1], [4]. These variations are larger than in healthy individuals [5] and preclude the possibility of obtaining a unique control algorithm that works for everyone. In consequence, most recent research efforts are focused on model personalization [1], [2], [6]–[14]. To avoid model identification, these approaches use patient-specific clinical variables like Total Daily Insulin (TDI), Insulin-to-Carbohydrate Ratio (CR) or body weight to individualize the controller's gain. Model Predictive Control (MPC) algorithms are individualized by using patient-specific model parameters or personalizing the MPC cost function weights [15], [16]. Adaptive algorithms (like run-to-run control) that adjust and individualize controller parameters have also been proposed [17]–[25]. It is worth remarking that in the aforementioned control-oriented models no intra-patient variability was embedded into the model structure.

Intra-subject variability is an additional important challenge for the AP. Subject's insulin requirements to control glycemia vary across the daytime [26], attributed to circadian changes in Glucose Tolerance (GT), i.e., the relative amount of glucose taken up by peripheral tissue [27], and S_I [28], which corresponds to the ability of insulin to stimulate glucose utilization and inhibit its production [29], regulating how sensitive is the body to the effects of insulin. This subject-specific variability is influenced by many factors like meals, stress, sleep architecture,

physical activity, rhythms of counterregulatory hormones, and quality of BG control [3], [8], [30]–[32]. Given that such factors ultimately may be reflected on the patient's S_I, intra-patient variability can be described by suitable modeling of circadian S_I variation [26]–[28], [31]. In this regard, intra-patient variations were included in the UVA/Padova metabolic simulator [33]–[35] by associating each *in-silico* subject with one of seven possible variability classes, assigned to a specific time-varying S_I profile [5], [36]. These profiles were created by modulating V_{mx}, which governs the insulin-dependent glucose utilization, and k_{p3}, which regulates the insulin action on the liver, as time-varying parameters. Similar approches were followed in [22], [37], where sinusoidal deviations of 20% amplitude over the nominal values related to insulin sensitivity and absorption were added for controller testing. In this way, the observed S_I variation of $\pm 30\%$ is included [28], but there is no consensus yet on how to model these variations.

Although S_I variations have been generally considered to test glucose controllers through extensive simulations, better closed-loop performance may be obtained if these variations were included in the controller synthesis stage. Several approaches have been considered in this matter. In [1], [9], the *in-silico* subjects of the UVA/Padova simulator are sorted in four groups according to the average value of their daily CR profile (related to each subject's S_I), with a personalized Linear Time Invariant (LTI) model associated with each group. This model is then used as a one-step ahead prediction model to synthesize a customized MPC. However, since LTI models are used, there is a significant loss of information regarding the patient's dynamics, considering its time-varying characteristics.

On a different approach, adaptive control systems consider intra-patient variations by embedding the model in the controller and adjusting controller parameters as experimental data reflects a time-variation in the model dynamics. Other adaptive control systems update the parameters of the model recursively as new data are collected from the system, and use the latest model in the controller [21], [24], or run-to-run control strategies to adapt basal insulin patterns [20], [23], [25], insulin boluses [7], [18], [19], [22], [38], or MPC cost functions [2]. Of these, the works of [18], [19] considered subject's S_I for assessing the controller's gain, but this S_I was determined using only some outputs, and therefore, does not characterize the insulin sensitivity of the virtual patient in the traditional sense [19]. On [23], [25] the algorithm is able to adjust intra- and inter-day S_I variations, by updating CR and basal insulin patterns according to perfomance indexes computed at the end of each day.

Another approach to cope with intra-patient variability is to compute tight-solution bounds on prediction models. In [32], [39], parametric variations over a glucose-insulin model are used to compute a solution envelope that is used as a prediction model in control structures like MPC. Instead, in [40], a Linear Parameter Varying (LPV) model *set* was obtained to cover both, S_I variations and dynamic uncertainties, for each patient. From a control design viewpoint, to "cover" intra-patient variations with bounded uncertainty is more conservative than to explicitly include them in the model. The latter embeds these time-varying dynamics in the controller, which could in theory [41], [42], lead to better performance.

S_I parametric variations embedded in the patient's model are considered in [43], where the Medtronic Virtual Patient (MVP) model is identified for ten different subjects based on closed-loop glucose-insulin data and the oral minimal model [44]. Intra-day variations in S_I related parameters were structured to change during three time-windows inside a 24-hour time period, assuming one value during the first and last time-windows and a different value during the second one. S_I variations were identified in six of the ten subjects of the study, presenting different starting times and segment duration among them.

Note that these approaches consider a specific S_I variation profile [43] or average daily S_I value [1], [4]. Considering that for some subjects parameters can present substantial differences over time, these models would not be able to follow or include such changes. Real-time parametric identification can help improve closed-loop performance. However, the ability of real-time identification algorithms to track time-varying parameters needs to be carefully assessed before their implementation for controller design.

A good control-oriented model should have a structure that allows a well-known, reliable, and numerically robust control synthesis technique to produce a controller that can be implemented in real-time. Considering the time-varying characteristics of the glucose regulation problem, LPV models are good candidates, and can result in LPV or switched LPV (or LTI) control strategies, that can yield better performance for the AP, as presented in [14], [45], [46]. In this regard, in [14], we presented a third-order LPV model that reflects the time-varying and non-linear nature of the glucose regulation problem by an average (over all subjects) structure, including a parameter dependent on the glucose level, which is measured in real-time.

Therefore, this work focuses on developing a model that reflects time-varying S_I variations within the model, while maintaining a simple structure that allows reliable and robust control synthesis techniques to be used. For this, an extension of [14] that includes S_I variations is developed, by introducing a second time-varying parameter to its low-order LPV structure. The model now includes intra- and inter-patient variations, and still preserves the possibility of personalizing it based on the 1800-rule, through a procedure that can be carried out in real patients in a non-invasive way.

The paper is organized as follows. In Section II the baseline LPV model [14] is described. Section III presents the procedure to obtain the LPV model with intra-patient variations. Section IV presents the open- and closed- loop evaluation of the model efficiency. Finally, conclusions are discussed in Section V.

II. Materials and Methods

The baseline control-oriented LPV model used in this work is the one developed in [14], [46] that is based on the UVA/Padova metabolic simulator [33]. It has a low-order structure akin to the one presented in [6], where the input corresponds to the subcutaneous insulin infusion (in pmol/min) and the output is the glucose concentration deviation (in mg/dl):

$$G(s) = k\frac{s+z}{(s+p_1)(s+p_2)(s+p_3)}\mathrm{e}^{-15s}. \tag{1}$$

An average model was first identified at a glucose concentration $g = 235$ mg/dl, where the 1800-rule is rendered correct for the nonlinear model [14], [46]. Then, its domain of validity was extended by allowing parameter p_1 to vary with g in order to fit the average Bandwith (BW) of the linearized models at different glucose values, keeping all other parameters fixed ($z = 0.1501$, $p_2 = 0.0138$ and $p_3 = 0.0143$). Pole $p_1(g)$ was approximated by the following piecewise-polynomial function:

$$p_1(g) = q_i\, g^3 + r_i\, g^2 + s_i\, g + t_i$$
$$\text{with} \quad i = \begin{cases} 1 & \text{if } g \geq 300 \\ 2 & \text{if } 110 \geq g < 300 \\ 3 & \text{if } 65 \geq g < 110 \\ 4 & \text{if } 59 \geq g < 65 \\ 5 & \text{if } g < 59 \end{cases} \tag{2}$$

and with coefficient values given in Table I.

In this way, a simple manner of replicating changes in the model's gain according to the glucose value was obtained, since the BW and Low-Frequency Gain (DC Gain) of the model are related by the time-varying parameter p_1.

The median glucose-dependent model (1) can then be tuned to a specific subject by adjusting parameter k with his/her TDI as follows. For each subject $\#j$, the LPV model at 235 mg/dl is excited with a 1 U insulin bolus and the value of k_j is determined so that the glucose drop matches the one predicted by the 1800-rule ($1800/TDI_j$). Here, it is worth remarking that parameter k_j is time-invariant, but specific to each subject.

A state-space representation of the personalized LPV model (defined as LPV$_g$ model) is given by:

$$\begin{aligned} \dot{x}(t) &= A(p_1)x(t) + Bu(t-\tau) \\ y(t) &= Cx(t) \end{aligned} \tag{3}$$

with $\tau = 15$ min, u and y the insulin delivery and glucose signals, and

$$\begin{aligned} A(p_1) = &\begin{bmatrix} 0 & 1 & 0 \\ 0 & 0 & 1 \\ 0 & -p_2p_3 & -(p_2+p_3) \end{bmatrix} \\ &+ p_1 \begin{bmatrix} 0 & 0 & 0 \\ 0 & 0 & 0 \\ -p_2p_3 & -(p_2+p_3) & -1 \end{bmatrix}, \\ B = &\begin{bmatrix} 0 & 0 & 1 \end{bmatrix}^T, \quad C = k_j \begin{bmatrix} z & 1 & 0 \end{bmatrix}. \end{aligned} \tag{4}$$

Note that the LPV$_g$ model is affine in parameter p_1, which is an advantageous characteristic for the design of LPV controllers [47]. Moreover, LPV$_g$ was compared to the UVA/Padova simulator in terms of the Root Mean Square Error (RMSE) and the ν-gap metric [48], [49], achieving better performance than control-oriented models presented previously in this field [3], [6], [45]. It is worth noting that this model was used for controller-design in a recent clinical trial, achieving promising results [50], [51].

TABLE I
PARAMETER VALUES OF $p_1(g)$ FROM (2)

i	q_i	r_i	s_i	t_i
1	0	0	-3.4321×10^{-6}	4.4706×10^{-3}
2	0	9.0580×10^{-8}	-5.3562×10^{-5}	1.1357×10^{-2}
3	-4.2382×10^{-8}	1.1402×10^{-5}	-9.1676×10^{-4}	2.5849×10^{-2}
4	0	1.7321×10^{-4}	-2.3080×10^{-2}	7.7121×10^{-1}
5	0	0	-2.8336×10^{-5}	1.4083×10^{-2}

III. PROPOSED LPV MODEL

A. Inclusion of Intra-Patient Variations

In this section, an extension of model (4) that includes intra-patient variability is developed — the LPV$_i$ model. The proposed structure is identified from linearizations of the UVA/Padova metabolic model around several operating points defined by steady-state glucose concentrations achieved by only accommodating the insulin infusion rate.

Glucose concentrations in the range [40, 400] mg/dl were considered to span the usual measurement range of CGM sensors, within a non-uniform grid. Since an average structure was pursued instead of specific S_I values, an Insulin Sensitivity Variation Factor ($S_{I,VF}$) was defined as $S_{I,VF} = S_I/S_{I,nom}$, where $S_{I,nom}$ could be considered as its average daily or basal [52] value. $S_{I,VF}$ was selected in the range $[0.4,\ 1.7]$ over a uniform grid with a step of 0.1, to cover the previously observed variations of $[40, 60]\%$ around the nominal subject-specific S_I [5], [22], [53].

For each subject, the operating points $(g_{op}, SI_{VF,op})$ were defined over each pair (g, SI_{VF}) on the grid. The insulin infusion rate was adjusted accordingly to achieve steady-state conditions at the glucose level g_{op} when parameters V_{mx} and k_{p3} were modulated by $SI_{VF,op}$. Then, as in [14], linearizations of the UVA/Padova model were obtained for each *in-silico* adult of the distribution version of the simulator.

Fig. 1 shows the average variation of the BW and DC Gain for LPV$_g$ and all *in-silico* adults linearized at different g and $S_{I,VF}$ values. Note that both BW and DC Gain coincide exactly at $S_{I,VF} = 1$.

Given that the DC Gain of model (1) is $\frac{kz}{p_1p_2p_3}$, and that the BW is independent of k, the LPV$_g$ model is expanded by making parameter k dependent on g and $S_{I,VF}$ as depicted in Fig. 2. Following this approach, variations of the model's gain due to S_I changes (see Fig. 1) can be reproduced, without affecting the previous BW fitting.

In this way, k is used to compensate both inter-patient variations through the 1800-rule and intra-patient variations by making k change according to a suitable S_I profile. The latter could be a general profile (such as those in [22], [36], [37]) or a profile obtained from clinical data using the pump/CGM index in [54], or through an estimation based on real-time measurements. This grants flexibility to the selected model structure, so it can be used together with the S_I profile that best suits subject-specific circadian variations in S_I, or even considering other factors that

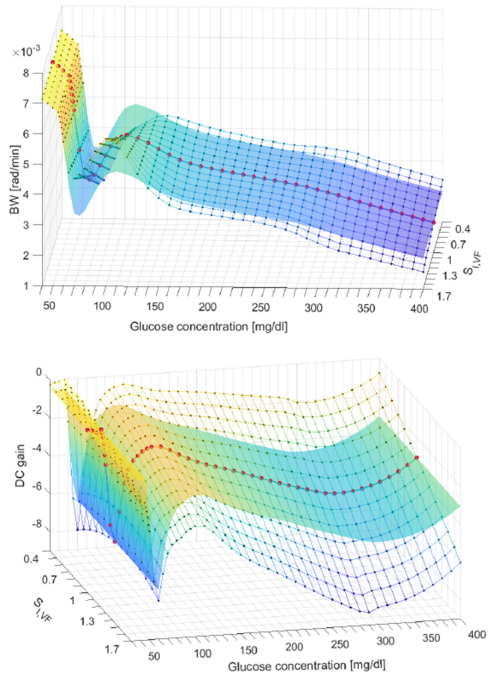

Fig. 1. BW (top) and DC Gain (bottom) of LPV$_g$ (smooth surface) for all *in-silico* adults from the UVA/Padova simulator linearized at different g and $\mathrm{S_I}$ values (gridded surface). The red dotted line indicates the BW at nominal $\mathrm{S_I}$.

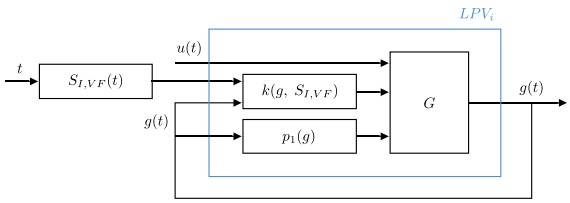

Fig. 2. Average LPV$_i$ model structure.

influence $\mathrm{S_I}$ such as physical exercise or stress [28], [30], [31], [55]–[57].

In order to characterize the dependence of parameter k on g and $\mathrm{S_{I,VF}}$, the definition of the DC Gain of model (1) is used. Here, the observed values for the DC Gain of the linearized models at each $(g, \mathrm{S_{I,VF}})$ pairs (defined as $\mathrm{DCG}_{NL}(g, \mathrm{S_{I,VF}})$), together with the constant parameters p_2, p_3 and $p_1(g)$ from (2), are used to compute an average value for parameter k, defined as k_{avg}:

$$k_{avg}(g, \mathrm{S_{I,VF}}) = \frac{p_2 p_3}{z} p_1(g) \mathrm{DCG}_{NL}(g, \mathrm{S_{I,VF}}) \qquad (5)$$

Then, the result was fitted using a piecewise polynomial function as indicated in the Appendix, and presented in Fig. 3.

Note that as shown in Fig. 1, there is an abrupt change at 60 mg/dl. The reason for this discontinuity is that the insulin-dependent glucose utilization in the UVA/Padova simulator is associated with a risk function that increases when glucose decreases below the subject's basal glucose concentration and saturates when glucose reaches 60 mg/dl. To avoid translating this artifact discontinuity to the glucose output, a smooth surface was fitted instead.

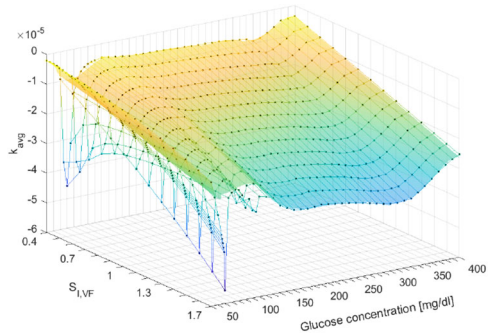

Fig. 3. Parameter k_{avg} for different values of g and $\mathrm{S_{I,VF}}$ (gridded surface) and piecewise polinomial function $k_{avg}(g, \mathrm{S_{I,VF}})$ (smooth surface).

In this way, the state-space representation of the average LPV$_i$ model is similar to (4), but now with the output matrix:

$$C = k_{avg}(g, \mathrm{S_{I,VF}}) \begin{bmatrix} z & 1 & 0 \end{bmatrix}. \qquad (6)$$

B. Model Personalization

In Section III, it was shown how k can be used to tackle intra-patient variability. In this Section, k is further tuned to reduce inter-patient uncertainty. This model personalization is carried out in a similar way as the one described in [14], i.e., by adjusting model's k using the 1800-rule.

In this case, a suitable gain $k^\star$ is computed as the gain that makes the LPV$_i$ model achieve the same glucose drop as the one predicted by the 1800-rule when excited with a 1 U insulin bolus at $g = 235$ mg/dl and $\mathrm{S_{I,VF}} = 1$. This point was selected since it was the one at which the 1800-rule was satisfied on average for all the *in-silico* adults [14]. A simple Proportional-Integral (PI) control loop, which modified k of the LPV$_i$ model until the model's glucose drop matched the one predicted by the 1800-rule, was used to obtain $k^\star$ for each adult.

Considering that for each subject the DC gain of the model at $g = 235$ mg/dl and $\mathrm{S_{I,VF}} = 1$ should be $k^\star$, a subject-specific scaling factor k_j is computed as $k_j = k^\star / k_{avg}(235, 1)$, where $k_{avg}(235, 1) = -1.822 \times 10^{-5}$. Then, a parameter $k_s(g, \mathrm{S_{I,VF}})$ is defined as $k_s = k_j k_{avg}$, with k_j given in Table II and k_{avg} the same fitted-surface of 3. Model personalization is thus achieved by replacing k_{avg} in (6) with parameter $k_s(g, \mathrm{S_{I,VF}})$. Note that this corresponds to a vertical shifting of the fitted k_{avg} surface.

Variations of $k_s(g, \mathrm{S_{I,VF}})$ for the average *in-silico* subject, and the most and least sensitive subjects are presented in Fig. 4. Note that the most sensitive subject (Adult #009), whose TDI is the lowest, is associated with the highest scaling factor k_j, and therefore, higher values of k_s (in module).

IV. Results and Discussion

A good simulation model, i.e., one that fits properly the experimental data, is not necessarily a good candidate to design

TABLE II
SCALING FACTOR k_j FOR EACH *IN-SILICO* ADULT

Adult	TDI [U/day]	$k^\star \times 10^{-5}$	k_j
1	42	-1.7888	0.9818
2	43	-1.7451	0.9578
3	52	-1.4343	0.7872
4	35	-2.1396	1.1743
5	40	-1.8650	1.0236
6	72	-1.0343	0.5677
8	52	-1.4379	0.7892
9	34	-2.2024	1.2088
10	47	-1.5919	0.8737
11	39.9	-1.8864	1.0354

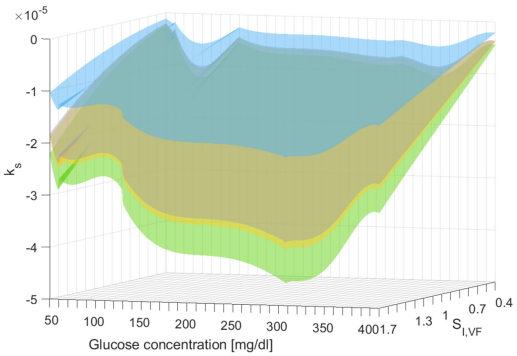

Fig. 4. k_{avg} (gray surface) and personalized k_s for the average subject (yellow surface), Adult #006 (blue surface) and Adult #009 (green surface).

controllers [58]. Therefore, in this section, a comparison of both LPV$_g$ and LPV$_i$ with respect to the UVA/Padova model is carried out not only for simulation (open-loop) purposes, but also for controller synthesis (closed-loop). No other models are considered here, since in [14] LPV$_g$ already showed lower closed- and open-loop errors than previous control-oriented models [3], [6], [45].

A. Open-Loop Comparison

Considering that S_I varies mostly during the day, the simulations are performed incorporating the time-varying profiles determined in [36]. First, the class 1 profile is analyzed, by maintaining the same S_I value during the day, but changing it's nominal value in the simulator. For each of the 10 *in-silico* subjects of the distribution version of the UVA/Padova simulator, an insulin bolus of 1 U was applied at different operating points to test the personalized LPV$_i$ and LPV$_g$ models in comparison with the UVA/Padova nonlinear simulator. Next, the other six profiles were considered.

1) Fixed S_I Values (Class 1): Fig. 5 presents the time-responses for Adult #009 (most sensitive subject) to a 1 U insulin bolus for multiple $S_{I,VF}$ values at basal glucose concentrations of 120, 180, and 240 mg/dl. Parameters p_1 and k_s variations for the LPV$_g$ and LPV$_i$ models are also depicted. Note that a better fit is achieved with LPV$_i$ than with LPV$_g$ for most $S_{I,VF}$ values. The reason is that only LPV$_i$ adjusts its gain to reflect changes in S_I. In addition, it is worth clarifying that despite the LPV$_i$ model is an extension of the LPV$_g$ model, its

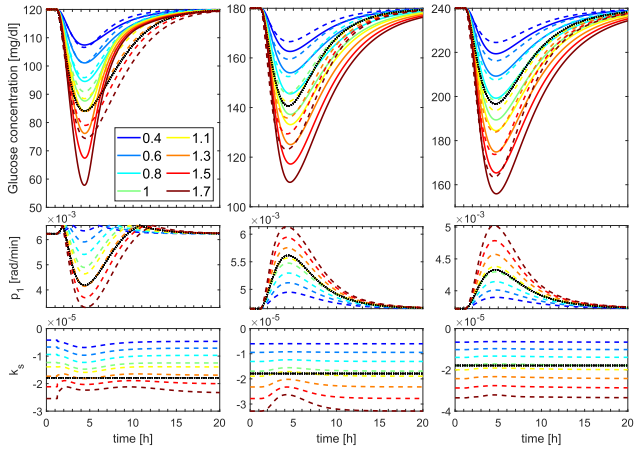

Fig. 5. Responses to a 1U insulin bolus starting from 120 mg/dl, 180 mg/dl and 240 mg/dl for Adult #009 at different $S_{I,VF}$ values for models LPV$_g$ (dotted black line), LPV$_i$ (dashed lines) and the UVA/Padova nonlinear model (solid lines). Top: Glucose drop. Middle: Evolution of parameter p_1. Bottom: Evolution of parameter k_s.

behavior for nominal insulin sensitivity ($S_{I,nom}$) is the same only at 235 mg/dl as an operating point, i.e., the glucose concentration at which they were both identified. For other glucose concentrations, the gain adjustment through variation of parameter $k_s(g, S_{I,VF})$ generates the differences between both models.

The RMSE between the time-responses of each LPV ($\boldsymbol{y_p}$) and the UVA/Padova model ($\boldsymbol{y}$), for each subject at each operating point on the (g,$S_{I,VF}$) grid, was computed according to the following equation:

$$\text{RMSE} = \frac{\|\boldsymbol{y_p} - \boldsymbol{y}\|_2}{\sqrt{n_t}} \tag{7}$$

where $\|\cdot\|_2$ represents the 2-norm, and n_t the number of points. In order to capture the complete glucose variation at each point, $n_t = 1200$ points with a sampling time of 1 minute, were selected. In Fig. 6, median values of the RMSE for all 10 *in-silico* adults at different g and $S_{I,VF}$ values are shown. Note that a lower RMSE can be obtained with LPV$_i$ than with LPV$_g$ for most glucose concentrations. Considering S_I variations, for the least sensitive case ($S_{I,VF} = 0.4$), LPV$_i$ outperforms LPV$_g$ for the whole glucose range. For $S_{I,nom}$ ($S_{I,VF} = 1$), both LPV models have approximately the same RMSE, except for glucose concentrations around 90–180 mg/dl, where the increased sensitivity of the UVA/Padova model is further adjusted by the variation of the k_s parameter in LPV$_i$. For a glucose concentration of 235 mg/dl, similar errors are observed since, as discussed before, at this point both models are equivalent. For the most sensitive case ($S_{I,VF} = 1.7$), LPV$_i$ has a similar RMSE as LPV$_g$ for $g < 140$ mg/dl, but at higher g values the difference in the DC Gain between both models becomes larger and LPV$_i$ provides a better fit.

2) Time-Varying S_I Profiles (Classes 2–7): Fig. 7 and 9 present the time responses for Adult #009 to three insulin boluses in the set $\{0.5,\ 1,\ 1.5\}$ U, applied at 7, 14, and 21 hours, respectively, for different profiles of S_I variation with a glucose operation point of 120 mg/dl. For these scenarios, the basal

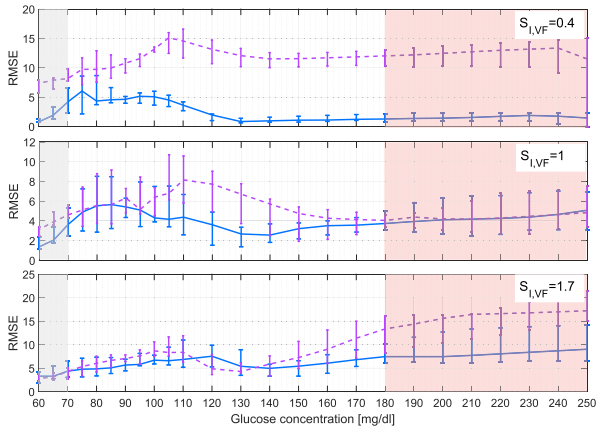

Fig. 6. Median RMSE between the time-responses of the personalized LPV$_g$ (violet dashed lines) and LPV$_i$ (blue solid lines), as compared with the UVA/Padova nonlinear model to an insulin bolus of 1 U for different $\mathrm{S_{I,VF}}$ values. Top: most resistant case ($\mathrm{S_{I,VF}} = 0.4$), middle: nominal case ($\mathrm{S_{I,VF}} = 1$), bottom: most sensitive case ($\mathrm{S_{I,VF}} = 1.7$). The vertical bars are limited by the 25th and 75th percentiles.

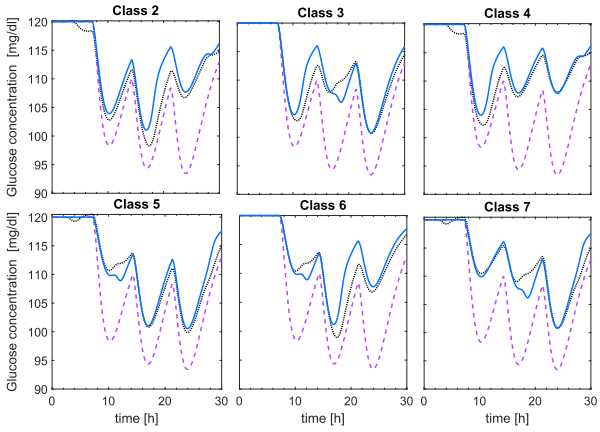

Fig. 7. Responses to three 0.5 U insulin boluses starting at 120 mg/dl for Adult #009 with different $\mathrm{S_I}$ profiles for models LPV$_g$ (dotted violet line), LPV$_i$ (solid blue lines) and the UVA/Padova nonlinear model (dotted black lines).

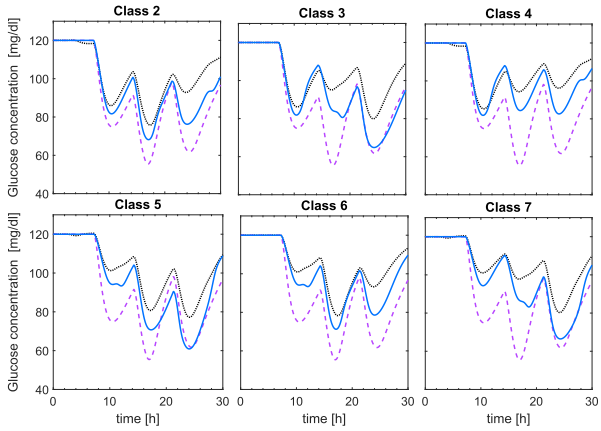

Fig. 8. Responses to three 1 U insulin boluses starting at 120 mg/dl for Adult #009 with different $\mathrm{S_I}$ profiles for models LPV$_g$ (dotted violet line), LPV$_i$ (solid blue lines) and the UVA/Padova nonlinear model (dotted black lines).

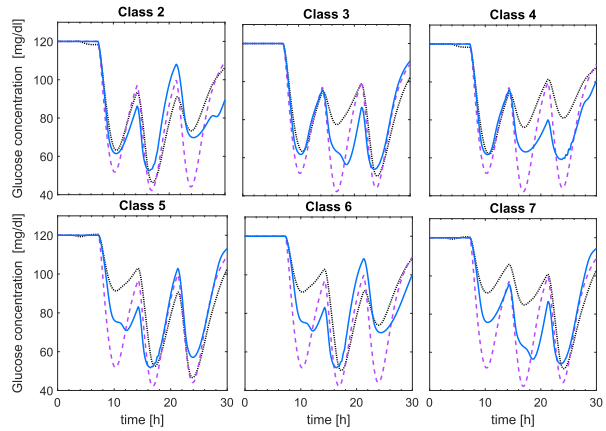

Fig. 9. Responses to three 1.5 U insulin boluses starting at 120 mg/dl for Adult #009 with different $\mathrm{S_I}$ profiles for models LPV$_g$ (dotted violet line), LPV$_i$ (solid blue lines) and the UVA/Padova nonlinear model (dotted black lines).

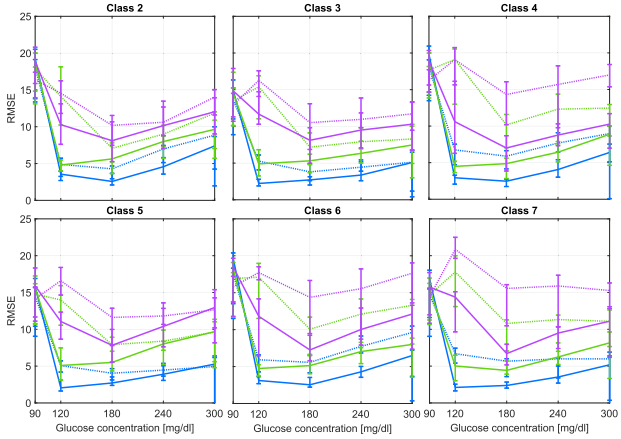

Fig. 10. Median RMSE between the time-responses of the personalized LPV$_g$ (dashed lines) and LPV$_i$ (solid lines), as compared with the UVA/Padova nonlinear model to three insulin boluses of 0.5 U (blue), 1.0 U (green) and 1.5 U (violet) for different $\mathrm{S_I}$ profiles. Vertical bars are limited by the 25th and 75th percentiles.

insulin infusion rates were accommodated to maintain steady-state conditions after $\mathrm{S_I}$ changes, as performed in [59]. In these cases, the LPV$_i$ model is able to reflect the $\mathrm{S_I}$ variation regardless of the $\mathrm{S_I}$ profile or the applied bolus, better than the LPV$_g$ model. In this way, the LPV$_i$ model obtains a more accurate representation of the UVA/Padova model, adapted to the subject's individual $\mathrm{S_I}$ profile. Additionally, the same scenario was tested at glucose operating points in the set {90, 180, 240, 300} mg/dl, obtaining the same results as for 120 mg/dl. These values were selected in order to span the complete glycemic range with the simulated glucose traces, bearing in mind that only insulin was considered as input.

The average RMSE between the time-responses of both LPV$_i$ and LPV$_g$ models and the UVA/Padova model is shown in Fig. 10. Note that for all $\mathrm{S_I}$ variation classes, a lower RMSE was obtained with the LPV$_i$ model than with the LPV$_g$ model.

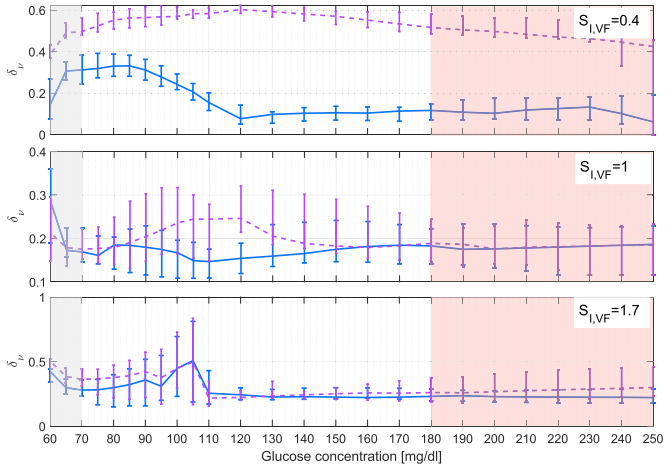

Fig. 11. Median ν-gap (δ_ν) between the linearizations of the UVA/Padova nonlinear model and models LPV$_g$ (violet dashed lines) and LPV$_i$ (blue solid lines) for different $\mathrm{S_{I,VF}}$ values. Top: most resistant case ($\mathrm{S_{I,VF}} = 0.4$), middle: nominal case ($\mathrm{S_{I,VF}} = 1$), bottom: most sensitive case ($\mathrm{S_{I,VF}} = 1.7$). The vertical bars are limited by the 25th and 75th percentiles.

B. Closed-Loop Comparison

In this case, the ν-gap distance [48], [49] between each personalized LPV model and the UVA/Padova model linearized at different points of the $(g, \mathrm{S_{I,VF}})$ grid is computed. This metric considers the distance (δ_ν) between two models regarding their achievable closed-loop performance, without having to design the controllers for each loop.

For LTI models, given a controller K and a model P_1, with K and P_1 transfer matrices, a performance measure/stability margin for the (stable) closed-loop system (P_1, K) is defined in [48], [49] as:

$$b_{P_1,K} = \left\| \begin{bmatrix} P_1 \\ I \end{bmatrix} (1 - KP_1)^{-1} \begin{bmatrix} -K & I \end{bmatrix} \right\|_\infty^{-1} \tag{8}$$

where $\|\cdot\|_\infty$ indicates the $\mathcal{H}_\infty$-norm. Here, larger values of $b_{P_1,K}$ correspond to better performance of the feedback system comprising P_1 and K. The difference between the performances of the nominal model and a perturbed one P_2 for the same controller K can be quantified through the ν-gap, i.e. $\delta_\nu(P_1, P_2)$, with $b_{P_2,K} \geq b_{P_1,K} - \delta_\nu(P_1, P_2)$. This indicates that the smaller $\delta_\nu(P_1, P_2)$ the closer their closed loop perfomances. Considering that if P_1 and P_2 represent alternate models of the same system (the UVA/Padova model and the LPV$_g$ or LPV$_i$ for example), a small $\delta_\nu(P_1, P_2)$ indicates that the differences between both models are negligible from a feedback perspective. Note that for its computation (see [48], [49]), only the plant models are required, and therefore their closed-loop performances can be compared without having to design the controller and compare on a one-by-one basis.

Fig. 11 presents the median ν-gap for all 10 adults for three different $\mathrm{S_{I,VF}}$ values, obtaining lower values with LPV$_i$, similar to the analysis presented in Section IV-A.

TABLE III
PERCENTAGE OF CASES OF MODEL IMPROVEMENT IN TERMS OF THE RMSE ($\%_{\mathrm{RMSE}}$) AND ν-GAP ($\%_{\nu\text{-GAP}}$). $\mathrm{H_{RMSE}}$ OR $\mathrm{H}_{\nu\text{-GAP}}$ EQUAL TO ONE INDICATE A SIGNIFICANT REDUCTION ON THE AVERAGE RMSE OR ν-GAP OBTAINED WITH LPV$_i$, CONSIDERING A 5% SIGNIFICANCE. TIME-VARYING $\mathrm{S_{I,VF}}$ VALUES CORRESPOND TO ALL $\mathrm{S_{I,VF}}$ PROFILES THAT WERE CONSIDERED

Adult # j	Constant $\mathrm{S_{I,VF}}$		Time-varying $\mathrm{S_{I,VF}}$		$\%_{\nu\text{-gap}}$	$\mathrm{h}_{\nu\text{-gap}}$
	$\%_{\mathrm{RMSE}}$	$\mathrm{h_{RMSE}}$	$\%_{\mathrm{RMSE}}$	$\mathrm{h_{RMSE}}$		
1	73.47	1	44.4	0	79.88	1
2	80.92	0	100.0	1	76.32	1
3	74.4	1	55.6	0	74.4	1
4	71.74	1	100	1	63.9	1
5	71.19	1	88.9	1	61.17	1
6	79.5	1	83.3	1	79.81	1
8	80.81	1	100.0	1	71.29	1
9	78.38	1	100.0	1	79.78	1
10	77.94	1	100.0	1	76.63	1
11	84.05	1	100.0	1	79.75	1
All	**77.17**	**1**	**87.22**	**1**	**73.82**	**1**

C. Overall Comparison

The difference between the RMSE and ν-gap obtained with both LPV models was computed for all (g,$\mathrm{S_{I,VF}}$) points considered in Section IV-A1, and all 10 *in-silico* adults, according to:

$$\delta_{\nu,d} = \delta_{\nu,\mathrm{LPV}_i} - \delta_{\nu,\mathrm{LPV}_g} \tag{9}$$

$$\mathrm{RMSE}_d = \mathrm{RMSE}_i - \mathrm{RMSE}_g \tag{10}$$

In this way, negative values of $\delta_{\nu,d}$ or RMSE_d indicate points where LPV$_i$ outperforms LPV$_g$.

A two-sampled t-test was carried out for each *in-silico* adult, to determine if the average RMSE obtained with LPV$_i$ is lower than the one obtained with LPV$_g$ at all (g,$\mathrm{S_{I,VF}}$) points and for all the time-varying $\mathrm{S_I}$ profiles considered. The same analysis was performed for the ν-gap to determine if including the $\mathrm{S_I}$ variation in the controller design stage could lead to a better closed-loop performance. Test results for each adult and the whole population (row 'All') are presented in Table III, along with the percentage of (g,$\mathrm{S_{I,VF}}$) points in which an improvement over LPV$_g$ is obtained, both in open- and closed-loop. According to these results, both open-loop and closed-loop metrics show an overall improvement using LPV$_i$ above 73.8%. It should be taken into account that the comparison measures were computed based on a simulated population and has an average significance. A better and more personalized result could be obtained by using clinical data from the $\mathrm{S_I}$ variations for a particular subject.

To recap, the main result here is the computation of an LPV structure, amenable to controller design. The procedure allows to include both inter- and intra-patient variations maintaining the time-varying characteristics of the system with a control-oriented focus based on real-time measurements and clinical data in a non-invasive way.

The model is able to accommodate variations in $\mathrm{S_I}$, which are the main cause of this variability. Therefore, the next step would be to couple the model with a $\mathrm{S_I}$ estimator from real-time measurements to include, for instance, exercise or stress influence on $\mathrm{S_I}$. Alternatively, this variability can be also represented as uncertainty bounds through an invalidation procedure, as the one carried out in [40], using field collected data.

TABLE IV
PARAMETER VALUES FOR $k_{avg}(g, \mathrm{S_{I,VF}})$ FROM (11)

n	1	2	3	4
$\lambda_{1,n}$	-7.641×10^{-03}	5.514×10^{-05}	8.356×10^{-05}	-2.011×10^{-05}
$\lambda_{2,n}$	9.024×10^{-05}	-1.186×10^{-06}	-2.645×10^{-06}	2.942×10^{-06}
$\lambda_{3,n}$	4.785×10^{-04}	3.262×10^{-05}	-5.145×10^{-05}	-1.352×10^{-04}
$\lambda_{4,n}$	-4.296×10^{-06}	-6.907×10^{-07}	8.635×10^{-07}	7.641×10^{-06}
$\lambda_{5,n}$	-3.971×10^{-07}	9.342×10^{-09}	2.470×10^{-08}	-1.323×10^{-07}
$\lambda_{6,n}$	-4.243×10^{-05}	3.838×10^{-06}	5.062×10^{-06}	8.139×10^{-05}
$\lambda_{7,n}$	1.225×10^{-08}	3.270×10^{-09}	-4.359×10^{-09}	-1.399×10^{-07}
$\lambda_{8,n}$	1.885×10^{-07}	-3.542×10^{-08}	-5.847×10^{-08}	-3.266×10^{-06}
$\lambda_{9,n}$	-1.966×10^{-10}	6.014×10^{-11}	0	2.696×10^{-08}
$\lambda_{10,n}$	7.718×10^{-10}	-3.175×10^{-11}	-7.066×10^{-11}	2.400×10^{-09}
$\lambda_{11,n}$	5.622×10^{-06}	-2.428×10^{-06}	0	-1.458×10^{-05}
$\lambda_{12,n}$	-1.153×10^{-11}	-5.211×10^{-12}	0	8.254×10^{-10}
$\lambda_{13,n}$	-1.546×10^{-08}	8.127×10^{-09}	0	3.713×10^{-07}
$\lambda_{14,n}$	-5.588×10^{-13}	3.937×10^{-14}	0	-1.575×10^{-11}

V. CONCLUSION

In this work, a low-order control-oriented model that includes intra-patient variations and generalizes previous works was proposed. This model depends on two parameters, $p_1(g)$ and $k_{avg}(g, \mathrm{S_{I,VF}})$, which in turn are functions of the glucose concentration and insulin sensitivity factors. These parameters can be computed in real-time and allow representing the nonlinear dynamics and the intra-patient variations. In addition, the model can also be easily personalized to reduce the inter-patient uncertainty by means of the well-known 1800-rule.

The use of $\mathrm{S_{I,VF}}$ allowed obtaining a general average structure that is not dependent on a particular model that describes changes in $\mathrm{S_I}$, i.e., it could be used in combination with any real-time $\mathrm{S_I}$ estimator (block $\mathrm{S_{I,VF}}(t)$ on Fig. 2). In this way, other factors influencing the subject's $\mathrm{S_I}$ like stress, exercise, meal size and composition, etc., could be considered in real time to obtain more robust and reliable controllers.

The proposed LPV_i was compared to the LPV_g model without the intra-patient variations in terms of its open- and closed-loop characteristics, by means of the RMSE and ν-gap, respectively. The proposed LPV_i showed better performance with smaller errors, highlighting the advantages of including $\mathrm{S_I}$ variations in the model's structure.

APPENDIX
AVERAGE PARAMETER-DEPENDENT GAIN

The piecewise polynomial function $k_{avg}(g, \mathrm{S_{I,VF}})$ is fitted as follows:

$$
\begin{aligned}
&k_{avg}(g,\ \mathrm{S_{I,VF}}) \\
&\quad = \lambda_{1,n} + \lambda_{2,n}\, g + \lambda_{3,n}\, \mathrm{S_{I,VF}} + \lambda_{4,n}\, g\, \mathrm{S_{I,VF}} \\
&\qquad + \lambda_{5,n}\, g^2 + \lambda_{6,n}\, {\mathrm{S_{I,VF}}}^2 + \lambda_{8,n}\, g\, {\mathrm{S_{I,VF}}}^2 + \lambda_{7,n}\, g^2\, \mathrm{S_{I,VF}} \\
&\qquad + \lambda_{9,n}\, g^2\, {\mathrm{S_{I,VF}}}^2 + \lambda_{10,n}\, g^3 + \lambda_{11,n}\, {\mathrm{S_{I,VF}}}^3 \\
&\qquad + \lambda_{12,n}\, g^3\, \mathrm{S_{I,VF}} + \lambda_{13,n}\, g\, {\mathrm{S_{I,VF}}}^3 + \lambda_{14,n}\, g^4 \\
&\text{with} \quad n = \begin{cases} 1 & \text{if } g \geq 300 \\ 2 & \text{if } 120 \leq g < 300 \\ 3 & \text{if } 45 \leq g < 120 \\ 4 & \text{if } g < 45 \end{cases}
\end{aligned}
\tag{11}
$$

with parameters values presented in Table IV.

REFERENCES

[1] M. Messori, G. P. Incremona, C. Cobelli, and L. Magni, "Individualized model predictive control for the artificial pancreas: In silico evaluation of closed-loop glucose control," *IEEE Control Syst.*, vol. 38, no. 1, pp. 86–104, Feb. 2018.

[2] P. Soru, G. De Nicolao, C. Toffanin, C. Dalla Man, C. Cobelli, L. Magni, and on behalf of the AP@home consortium, "MPC based artificial pancreas : Strategies for individualization and meal compensation," *Annu. Rev. Control*, vol. 36, pp. 118–128, 2012.

[3] J. Lee, E. Dassau, D. Seborg, and F. J. Doyle III, "Model-based personalization scheme of an artificial pancreas for type 1 diabetes applications," in *Proc. Amer. Control Conf.*, 2013, pp. 2911–2916.

[4] L. M. Huyett, E. Dassau, H. C. Zisser, and F. J. Doyle III, "Glucose sensor dynamics and the artificial pancreas: The impact of lag on sensor measurement and controller performance," *IEEE Control Syst.*, vol. 38, no. 1, pp. 30–46, Feb. 2018.

[5] L. Hinshaw *et al.*, "Diurnal pattern of insulin action in type 1 diabetes implications for a closed-loop system," *Diabetes*, vol. 62, no. 7, pp. 2223–2229, 2013.

[6] K. van Heusden, E. Dassau, H. C. Zisser, D. E. Seborg, and F. J. Doyle III, "Control-relevant models for glucose control using *a priori* patient characteristics," *IEEE Trans. Biomed. Eng.*, vol. 59, no. 7, pp. 1839–1849, Jul. 2012.

[7] C. Toffanin, S. Del Favero, E. Aiello, M. Messori, C. Cobelli, and L. Magni, "Glucose-insulin model identified in free-living conditions for hypoglycaemia prevention," *J. Process Control*, vol. 64, pp. 27–36, 2018.

[8] C. Toffanin, H. Zisser, F. J. Doyle III, and E. Dassau, "Dynamic insulin on board: Incorporation of circadian insulin sensitivity variation." *J. Diabetes Sci. Technol.*, vol. 7, no. 4, pp. 928–940, 2013.

[9] M. Messori, M. Ellis, C. Cobelli, P. D. Christofides, and L. Magni, "Improved postprandial glucose control with a customized model predictive controller," in *Proc. Amer. Control Conf.*, Jul. 2015, pp. 5108–5115.

[10] M. Messori, C. Toffanin, S. Del Favero, G. De Nicolao, C. Cobelli, and L. Magni, "Model individualization for artificial pancreas," *Comput. methods and programs biomedicine*, 2016.

[11] I. Hajizadeh *et al.*, "Multivariable recursive subspace identification with application to artificial pancreas systems," *IFAC-PapersOnLine*, vol. 50, no. 1, pp. 886–891, 2017.

[12] I. Contreras, S. Oviedo, M. Vettoretti, R. Visentin, and J. Vehí, "Personalized blood glucose prediction: A hybrid approach using grammatical evolution and physiological models," *PloS One*, vol. 12, no. 11, 2017, Art. no. e0187754.

[13] P. Colmegna, R. S. Sánchez-Peña, R. Gondhalekar, E. Dassau, and F. J. Doyle III, "Switched LPV glucose control in type 1 diabetes," *IEEE Trans. Biomed. Eng.*, vol. 63, no. 6, pp. 1192–1200, Jun. 2016.

[14] P. Colmegna, R. Sánchez-Peña, and R. Gondhalekar, "Linear parameter-varying model to design control laws for an artificial pancreas," *Biomed. Signal Process. Control*, vol. 40, pp. 204–213, Feb. 2018.

[15] L. Magni *et al.*, "Evaluating the efficacy of closed-loop glucose regulation via control-variability grid analysis," *J. Diabetes Sci. Technol.*, vol. 2, no. 4, pp. 630–635, Jul. 2008.

[16] A. Haidar, "The artificial pancreas: How closed-loop control is revolutionizing diabetes," *IEEE Control Syst.*, vol. 36, no. 5, pp. 28–47, Oct. 2016.

[17] L. Magni *et al.*, "Run-to-run tuning of model predictive control for type 1 diabetes subjects: in silico trial," *J. Diabetes Sci. Technol.,* vol. 3, no. 5, pp. 1091–1098, 2009.

[18] H. Zisser, L. Jovanovic, F. Doyle III, P. Ospina, and C. Owens, "Run-to-run control of meal-related insulin dosing," *Diabetes Technol. Therapeutics*, vol. 7, no. 1, pp. 48–57, 2005.

[19] C. Owens, H. Zisser, L. Jovanovic, B. Srinivasan, D. Bonvin, and F. J. Doyle, "Run-to-run control of blood glucose concentrations for people with type 1 diabetes mellitus," *IEEE Trans. Biomed. Eng.*, vol. 53, no. 6, pp. 996–1005, 2006.

[20] C. C. Palerm, H. Zisser, L. Jovanovič, and F. J. Doyle III, "A run-to-run control strategy to adjust basal insulin infusion rates in type 1 diabetes," *J. Process Control*, vol. 18, pp. 258–265, 2008.

[21] K. Turksoy and A. Cinar, "Adaptive control of artificial pancreas systems-a review," *J. Healthcare Eng.*, vol. 5, no. 1, pp. 1–22, 2014.

[22] P. Herrero *et al.*, "Method for automatic adjustment of an insulin bolus calculator: In silico robustness evaluation under intra-day variability," *Comput. Methods Programs Biomed.*, vol. 119, no. 1, pp. 1–8, 2015.

[23] C. Toffanin, M. Messori, C. Cobelli, and L. Magni, "Automatic adaptation of basal therapy for type 1 diabetic patients: a run-to-run approach," *Biomed. Signal Process. Control*, vol. 31, pp. 539–549, 2017.

[24] A. Nath, D. Deb, R. Dey, and S. Das, "Blood glucose regulation in type 1 diabetic patients: an adaptive parametric compensation control-based approach," *IET Syst. Biol.*, vol. 12, no. 5, pp. 219–225, 2018.

[25] C. Toffanin, R. Visentin, M. Messori, F. D. Palma, L. Magni, and C. Cobelli, "Toward a run-to-run adaptive artificial pancreas: In silico results," *IEEE Trans. Biomed. Eng.*, vol. 65, no. 3, pp. 479–488, Mar. 2018.

[26] E. Van Cauter, K. S. Polonsky, and A. J. Scheen, "Roles of circadian rhythmicity and sleep in human glucose regulation," *Endocrine Rev.*, vol. 18, no. 5, pp. 716–738, 1997.

[27] S. E. La Fleur, "Daily rhythms in glucose metabolism: Suprachiasmatic nucleus output to peripheral tissue," *J. Neuroendocrinology*, vol. 15, no. 3, pp. 315–322, 2003.

[28] E. Haus, "Chronobiology in the endocrine system," *Adv. Drug Del. Rev.*, vol. 59, no. 9, pp. 985–1014, 2007.

[29] C. Cobelli, C. D. Man, M. Schiavon, A. Basu, and Y. C. Kudva, U.S. Patent No. 9,486,172. Washington, DC: U.S. Patent and Trademark Office. 2016.

[30] S. Oviedo, J. Vehí, R. Calm, and J. Armengol, "A review of personalized blood glucose prediction strategies for t1dm patients," *Int. J. Numerical Methods Biomed. Eng.*, vol. 33, no. 6, pp. e2833–n/a, 2017.

[31] M. Moscoso-Vásquez, P. Colmegna, and R. Sánchez-Peña, "Intra-patient dynamic variations in type 1 diabetes: A review," in *Proc. IEEE Conf. Control Appl.*, Sep. 2016, pp. 416–421.

[32] D. de Pereda, S. Romero-Vivo, B. Ricarte, and J. Bondia, "On the prediction of glucose concentration under intra-patient variability in type 1 diabetes: A monotone systems approach," *Comput. Methods Programs Biomed.*, vol. 108, no. 3, pp. 993–1001, 2012.

[33] C. Dalla Man, F. Micheletto, D. Lv, M. Breton, B. P. Kovatchev, and C. Cobelli, "The UVA/Padova type 1 diabetes simulator: New features," *J. Diabetes Sci. Technol.*, vol. 8, no. 1, pp. 26–34, Jan. 2014.

[34] B. P. Kovatchev, M. Breton, C. D. Man, and C. Cobelli, "In silico preclinical trials: A proof of concept in closed-loop control of type 1 diabetes," *J. Diabetes Sci. Technol.*, vol. 3, no. 1, pp. 44–55, 2009.

[35] R. Visentin *et al.*, "The UVA/Padova type 1 diabetes simulator goes from single meal to single day," *J. Diabetes Sci. Technol.*, vol. 12, no. 2, pp. 273–281, 2018.

[36] R. Visentin, C. Dalla Man, Y. C. Kudva, A. Basu, and C. Cobelli, "Circadian variability of insulin sensitivity: Physiological input for in silico artificial pancreas," *Diabetes Technol. Therapeutics*, vol. 17, no. 1, pp. 1–7, 2015.

[37] F. León-Vargas, F. Garelli, H. D. Battista, and J. Vehí, "Postprandial response improvement via safety layer in closed-loop blood glucose controllers," *Biomed. Signal Process. Control*, vol. 16, pp. 80–87, 2015.

[38] P. Herrero, P. Pesl, M. Reddy, N. Oliver, P. Georgiou, and C. Toumazou, "Advanced insulin bolus advisor based on run-to-run control and case-based reasoning," *IEEE J. Biomed. Health Informat.*, vol. 19, no. 3, pp. 1087–1096, May 2015.

[39] A. J. Laguna, P. Rossetti, F. J. Ampudia-Blasco, J. Vehí, and J. Bondia, "Identification of intra-patient variability in the postprandial response of patients with type 1 diabetes," *Biomed. Signal Process. Control*, vol. 12, no. 1, pp. 39–46, 2014.

[40] F. Bianchi, M. Moscoso-Vásquez, P. Colmegna, and R. Sánchez-Peña, "Invalidation and low-order model set for artificial pancreas robust control design," *J. Process Control*, vol. 76, pp. 133–140, 2019, (Special issue on *Advances in Artificial Pancreas Control Systems*).

[41] K. Zhou, J. C. Doyle, and K. Glover, *Robust and Optimal Control*. New Jersey: Prentice–Hall, vol. 40, 1996.

[42] R. S. Sánchez Peña and M. Sznaier, *Robust Systems Theory and Applications*. Hoboken, NJ, USA: Wiley, 1998.

[43] S. S. Kanderian, S. Weinzimer, G. Voskanyan, and G. M. Steil, "Identification of intraday metabolic profiles during closed-loop glucose control in individuals with type 1 diabetes," *J. Diabetes Sci. Technol.*, vol. 3, no. 5, pp. 1047–1057, 2009.

[44] R. N. Bergman, L. S. Phillips, and C. Cobelli, "Physiologic evaluation of factors controlling glucose tolerance in man: Measurement of insulin sensitivity and beta-cell glucose sensitivity from the response to intravenous glucose." *J. Clinical Investigation*, vol. 68, no. 6, pp. 1456–1467, 1981.

[45] P. Colmegna, R. S. Sánchez-Peña, R. Gondhalekar, E. Dassau, and F. J. Doyle III, "Switched LPV glucose control in type 1 diabetes," *IEEE Trans. Biomed. Eng.*, vol. 63, no. 6, pp. 1192–1200, 2016.

[46] P. Colmegna, R. S. Sánchez-Peña, R. Gondhalekar, E. Dassau, and F. J. Doyle III, "Reducing glucose variability due to meals and postprandial exercise in T1DM using switched LPV control: In silico studies," *J. Diabetes Sci. Technol.*, vol. 10, no. 3, pp. 744–753, 2016.

[47] R. Tóth, *Modeling and Identification of Linear Parameter-Varying Systems*. Berlin, Germany: Springer, 2010, vol. 403.

[48] G. Vinnicombe, *Uncertainty and Feedback: $\mathcal{H}_\infty$ Loop-shaping and ν-gap metric*. London: Imperial College Press, 2001.

[49] G. Vinnicombe, "Frequency domain uncertainty and the graph topology," *IEEE Trans. Autom. Control*, vol. 38, no. 9, pp. 1371–1383, Sep. 1993.

[50] P. Colmegna, F. Garelli, H. D. Battista, and R. Sánchez-Peña, "Automatic regulatory control in type 1 diabetes without carbohydrate counting," *Control Eng. Pract.*, vol. 74, pp. 22–32, 2018.

[51] R. Sánchez-Peña *et al.*, "Artificial pancreas: Clinical study in latin america without premeal insulin boluses," *J. Diabetes Sci. Technol.*, vol. 12, no. 5, pp. 914–925, 2018.

[52] S. D. Patek *et al.*, "Empirical representation of blood glucose variability in a compartmental model," in *Prediction Methods for Blood Glucose Concentration*. Berlin, Germany: Springer, 2016, pp. 133–157.

[53] F. León-Vargas, F. Garelli, H. De Battista, and J. Vehí, "Postprandial blood glucose control using a hybrid adaptive PD controller with insulin-on-board limitation," *Biomed. Signal Process. Control*, vol. 8, no. 6, pp. 724–732, 2013.

[54] M. Schiavon, C. D. Man, Y. C. Kudva, A. Basu, and C. Cobelli, "Quantitative estimation of insulin sensitivity in type 1 diabetic subjects wearing a sensor augmented insulin pump," *Diabetes Care*, vol. 37, no. 5, pp. 39–49, 2013.

[55] M. Schiavon *et al.*, "Postprandial glucose fluxes and insulin sensitivity during exercise: A study in healthy individuals," *Amer. J. Physiol. Endocrinology Metabolism*, vol. 305, no. 4, pp. E557–566, 2013.

[56] K. Turksoy, L. Quinn, E. Littlejohn, and A. Cinar, "Multivariable adaptive identification and control for artificial pancreas systems," *IEEE Trans. Biomed. Eng.*, vol. 61, no. 3, pp. 883–891, Mar. 2014.

[57] R. Basu, M. L. Johnson, Y. C. Kudva, and A. Basu, "Exercise, hypoglycemia, and type 1 diabetes," *Diabetes Technol. Therapeutics*, vol. 16, no. 6, pp. 331–337, 2014.

[58] R. Sánchez-Peña and F. Bianchi, "Model selection: from LTI to switched-LPV," in *Proc. Amer. Control Conf.*, 2012, pp. 1561–1566.

[59] N. Rosales, H. De Battista, J. Vehí, and F. Garelli, "Open-loop glucose control: Automatic IOB-based super-bolus feature for commercial insulin pumps," *Comput. Methods Programs Biomedicine*, vol. 159, pp. 145–158, 2018.